ENVIRONMENTAL EFFECTS ON HIGH TEMPERATURE FATIGUE OF CARBON-POLYIMIDE TEXTILE COMPOSITES FOR AIRCRAFT APPLICATIONS

F. Foti[1], M. Gigliotti[1], Y. Pannier[1] and D. Mellier[1]

[1]Physics and Mechanics of Materials Department
Institut P', CNRS, University of Poitiers, ISAE-ENSMA, UPR 3346
1, avenue Clément Ader, BP 40109 F86961
FUTUROSCOPE CHASSENEUIL Cedex, FRANCE
E-mail: federico.foti@ensma.fr, Web Page: http://www.ensma.fr/

Keywords: textile carbon-polyimide composite, fatigue, environmental effect, µCT

Abstract
The present work focuses on "multi-physical" fatigue of 8HS woven $[45]_6$ carbon HTS40 carbon fiber/polyimide matrix composite samples. Fatigue tests are performed under controlled environment (2 bar O_2, 2 bar N_2) at 250° by using a specific experimental setup developed at PPRIME Institute. Digital Image Correlation (DIC) and µCT scans are used, respectively, to measure strain at the sample surface and for damage assessment. Comparatively to an inert environment (N_2), it is shown that an oxidizing environment (O_2) affects significantly damage kinetics and degradation.

1. Introduction

In the next future, the employment of organic matrix/carbon fiber composites (OMC) is foreseen for the realization of "hot" structures: these parts may be subjected, in service, to mechanical fatigue (e.g. fan blades turbo-engines), thermal cycling and thermo-mechanical fatigue (e.g. aircraft structural parts).
Though there is a consistent literature concerning the fatigue behavior of woven composites (see, for instance, [1-5]), polymer oxidation ([6, 7]) and about the thermal cycling of woven composites [8], the interaction between fatigue and environmental degradation at high temperature has been poorly explored. For these materials under such conditions, the presence of an oxidizing environment, for instance, may lead to the acceleration of the kinetics of damage onset and development due to coupled effect of mechanical stress and thermal oxidation of the polymer matrix.
Coupling between environmental and mechanical (viscoelastic, viscoplastic) behavior of the polymer matrix at high temperatures also deserves to be studied.
The long-term aim of this study is to provide some tools - both experimental and numerical - to strengthen the understanding and the modeling of the mechanics/damage/environment coupling and to provide tools to predict durability of composites.
In particular, this work aims at characterizing and modelling the thermo mechanical behavior, the onset and the development of damage related to cyclic mechanical mechanisms (fatigue) under controlled (temperature and gas) environment.

Excerpt from ISBN 978-3-00-053387-7

2. Specimens and experimental setup

8HS HTS40 carbon fiber/polyimide matrix $[45]_6$ specimens (samples dimensions: 170mm x 15mm x 2mm) are cut from a $[0]_6$ plate provided by Aircelle, SAFRAN Group. These samples (off-axis samples) are chosen due to their ability to enhance the matrix oxidation effect on the results. The glass transition temperature, T_g, of the matrix is equal to around 320°C. This material is expected to sustain in-service conditions up to around 250°C.
Fig. 1 shows the COMPTINN experimental setup, specifically developed in order to perform fatigue tests under controlled environment. An INSTRON 1251 hydraulic fatigue machine (F_{max}: 50 kN) is equipped with an aging chamber including a control of temperature and gas pressure (T_{max}: 350° C, p_{max}: 5 bar, environment: air, O_2, N_2, …). A system for gas supply and an electronic control heating is installed around the machine; this facility allows carrying out traction and fatigue test in controlled environment, achieving a maximal temperature of 350°C and a maximal gas pressure of 5 bar.

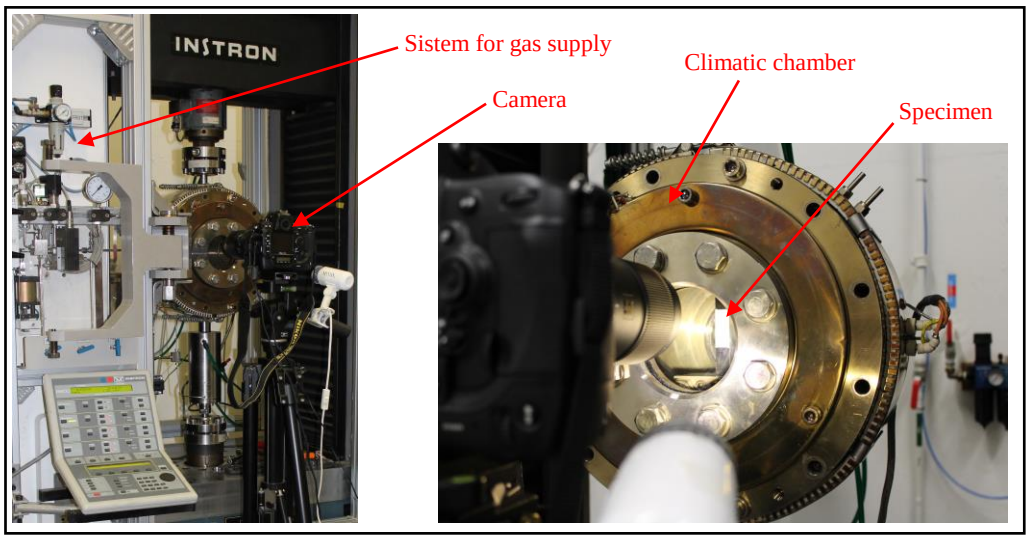

Figure 1. COMPTINN' experimental setup: INSTRON 1251 fatigue setup equipped with an environmental climatic chamber – available at the PPRIME institute

Since tests are performed at high temperature, the samples standing in a closed environmental chamber, non-contact measure method must be employed. Full field digital image correlation (DIC) method is used to measure sample strain during the test: a high temperature resistant (max usage temperature: 650°C) speckle pattern sprayed on one surface of the specimens is employed. During the tests, a series of pictures with a resolution of around 7 µm/pixel, at a frequency of 6 seconds each, are taken using a D3X Nikon. Starting from these pictures, deformations in longitudinal and trasversal directions are computed using CORRELA, a software dedicated to the digital image correlation developed at the PPRIME institute ([9]).
µCT scans are used to have a complete description of the damage scenario of the specimens. The RX Solution® (Fig. 2) X-Ray micro Computed Tomography available at the PPRIME Institute allows performing µCT scans with a resolution of 8,78µm using a voltage of 60kV and a current of 139µA on the tested samples. After the scans, image processing allows to semi-automatically find and evaluate damages inside the specimens. Image processing is performed using Avizo9®, a commercial software giving the possibility to carry out segmentation process of the damaged specimen [10].

Excerpt from ISBN 978-3-00-053387-7

3. Results of the fatigue tests

Two preliminary quasi-static tensile test at 250°C are carried out in order to decide the mechanical parameters for the fatigue test. The average failure stress, σ_{ult}, is around 140MPa, which corresponds to the maximum stress achieved during the tensile test.
Fatigue tests are performed using a maximal load level $\sigma_{max} = 0.7\ \sigma_{ult}$, a stress ratio $R = 0.1$ and a frequency $f = 2$Hz. The fatigue tests are periodically cut off (around 20 times) to perform slow load/unload cycles for DIC measures: samples are also periodically (4 times) removed from the test rig and subjected to ex-situ µCT scans.

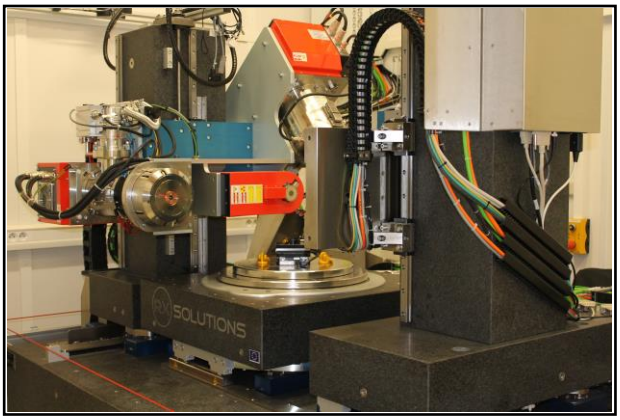

Figure 2. RX Solution® X-Ray micro Computed Tomography facility – available at the Pprime institute

Fatigue tests were carried out at 250°C under two different environmental conditions: the 2 bar O_2 environment is strongly aggressive ([11]) and should favor matrix degradation; the 2 bar N_2 is inert and may serve as a reference environment.

3.1. Results of DIC measures

DIC strain measures on sample surface allow characterizing the macroscopic mechanical behavior of the samples and its evolution with fatigue.
Shear deformation γ_{xy} and shear stress τ_{xy} are determined by using Eq. 1 and Eq. 2, where ε_y is the longitudinal strain, ε_x is the transversal strain obtained from DIC and σ_y is the longitudinal stress applied to the specimens obtained from the datasheet of the fatigue machine.

$$\gamma_{xy} = -(\varepsilon_y - \varepsilon_x). \quad (1)$$

$$\tau_{xy} = |\sigma_y|/2 \quad (2)$$

Fig. 3 shows the shear deformation γ_{xy} of the specimen tested in 2 bar of N_2 after 120k cycles, when loaded at σ_{max}. The CORRELA deformation field is not uniform because the noise and the sample's features (weave geometry and cracks). A mathematical mean of the pixels composing each DIC image is calculated in order to obtain a single deformation values of the specimen for each level of stress.
As it can be seen in Fig. 4, two variables could be taken to characterize the sample stress-strain plot: the secant shear modulus (G_{sec}, [*GPa*]) and the hysteresis area (A, [J/mm^3]).

Excerpt from ISBN 978-3-00-053387-7

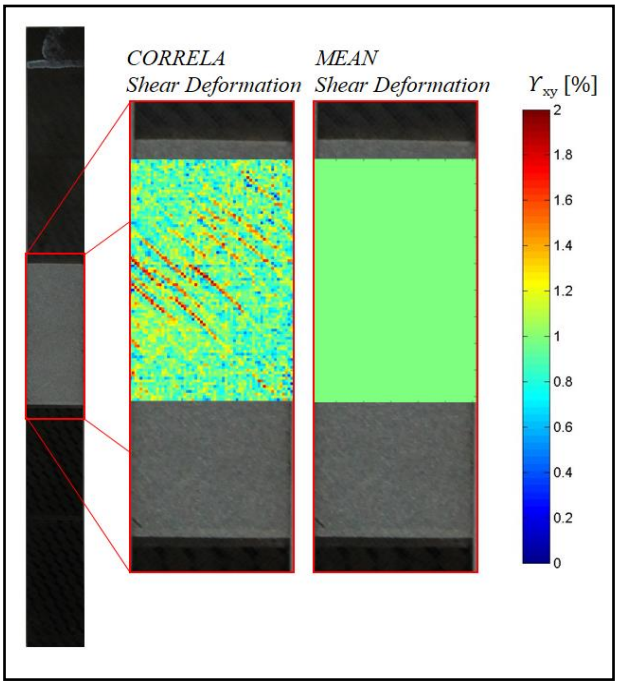

Figure 3. CORRELA shear deformation field (γ_{xy}) and mean of the same deformation field at σ_{max}

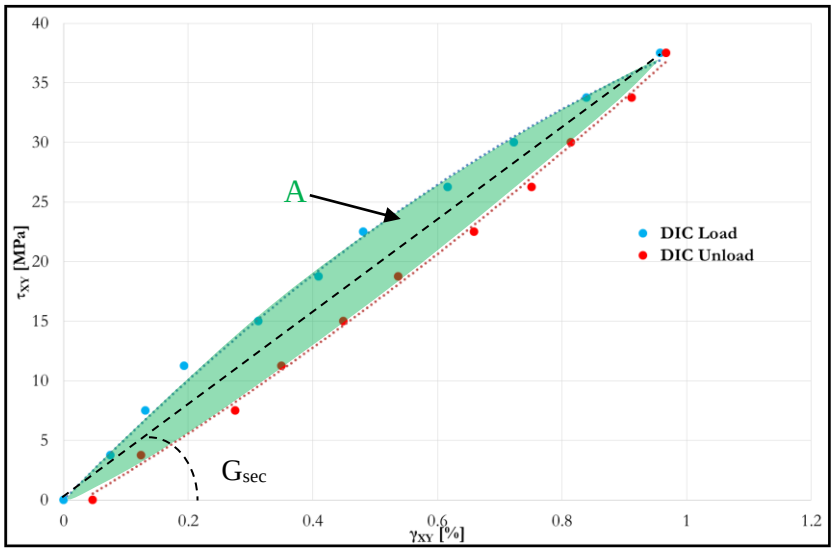

Figure 4. Typical stress-strain plot: secant shear modulus and hysteresis area.

Fig. 5 and Fig. 6 illustrate the evolution of G_{sec} and A as a function of the number of cylces for the two tested conditions. Failure of the 2 bar O_2 sample occurs at 550k cycles, while the 2 bar N_2 sample has not failed after 1M cycles.

Fig. 5 shows that, for both conditions, A values decrease of around 90% after 20k cycles. This decrease is possibly related to both stabilization of matrix viscoelastic hysteresis loops [12] at 250°C and the development of rapidly accumulating matrix cracking in the specimen ([4, 13, 14]). For the 2 bar N_2 sample, these stabilized values are kept until the end of the fatigue test. For the 2 bar O_2 sample, an increase of the A values is noted after 400k cycles, preceding sample failure. This rise can be related [13] to the increasingly non-linearity of the hysteresis loops due to the increase of fatigue damage.

Excerpt from ISBN 978-3-00-053387-7

Fig. 6 shows that G_{sec} values increase of around 185% after 50k cycles, for both experimental conditions; this shoud be related to stabilization of hysteresis loops. G_{sec} values are costant up to the end of the fatigue test for the 2 bar N_2, while tend decrease for O_2 starting from 300k cycles, with a sudden drop before failure. The evolution of apparent sample behavior is clearly affected by the environment which plays a role on matrix degradation (antiplastification, embrittlement [6]), onset and propagation of fibre/matrix debonding ([11]).

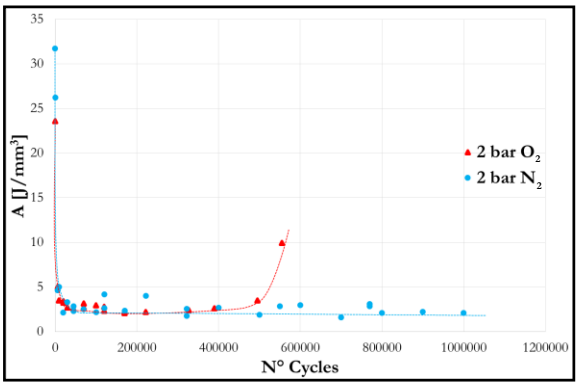

Figure 5. Hysteresis area (A) evolution during fatigue test, as a function of the number of cylces

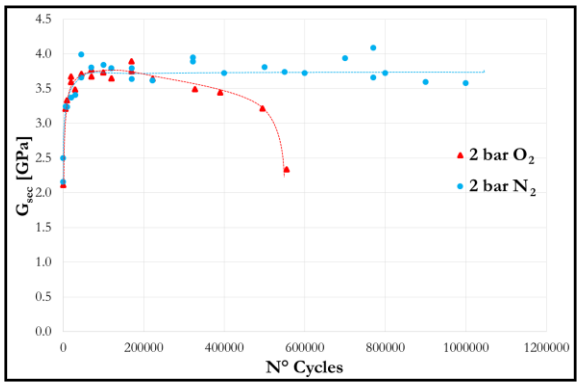

Figure 6. Secant shear modulus (G_{sec}) evolution during fatigue test, as a function of the number of cylces

3.2 Results of µCT scans

In order to better identify the physical mechanisms (damage, degradation …) responsible for the behavior observed at the macroscopic sample scale, µCT scans are carried out on interrupted fatigue samples. These observations are useful to elucidate the chronology of damage/degradation onset and development and to detect the sites/scale at which such phenomena take place.

Fig. 7 illustrates the steps of the crack segmentation process. The filters used to perform the segmentation allow the identification of the cracks starting from the grey level of the cracks (generally darker then the resin and the tows), the path of the cracks and the gradient of the grey level along the 3D images. The total damaged volume is then evaluated by applying the same process to the whole scanned sample volume. Fig. 7 shows that, in general, several types of damage occur during sample fatigue: cracks along the two fibers direction (in blue and green) appear inside all the plies, while cracks oriented in the direction perpendicular to the load direction (red), affect the resin rich regions only in the exterior plies.

Fig. 8 shows the total damaged volume ratio (D) defined as the total damaged volume divided by the total scanned volume as a function of the number of cycles for the two specimens. The indicator D does not discriminate between different types of cracks and, as one can see, its evolution is different for the two specimens: for the 2 bar N_2 sample the evolution of D shows a slight rise, while a major rise is observed for the the 2 bar O_2 sample.

The manual fitting of measures in Fig. 8 shows the begin of the acceleration of the damage process in the 2 bar O_2 sample at approximately 300k cycles. Results in Fig. 8 are in agreement with the G_{sec} evolution illustrated in Fig. 6 and support the existence of a good correlation between G_{sec} and D.

By looking at the damage distribution along the samples and in different plies it can be seen that, for both specimens, the major contribution to D comes from cracks situated on the external plies and that the morphology of the cracks depends on their location along the thickness.

Fig. 9 shows segmentation results for the 2 bar O_2 sample after 550k cycles: cracks located in the external plies are longer and more numerous than cracks located in internal plies. Moreover, in the internal plies, cracks propagate mainly close to the specimen edge, while, in superficial plies, several

Excerpt from ISBN 978-3-00-053387-7

cracks spread over the whole sample width; some cracks are not connected to the edge. The amount of cracks in internal plies is low up to 170k cycles comparatively to that measured in exterior plies. Cracks close to the internal plies edges are short (and barely visible) until 170k cycles, while long cracks on the surfaces are easily visible since 20k cycles. Since the environment affects primarily the external sample surfaces, this scenario reflects the high impact of the environment on crack morphology, density and propagation in the 2 bar O_2 sample.

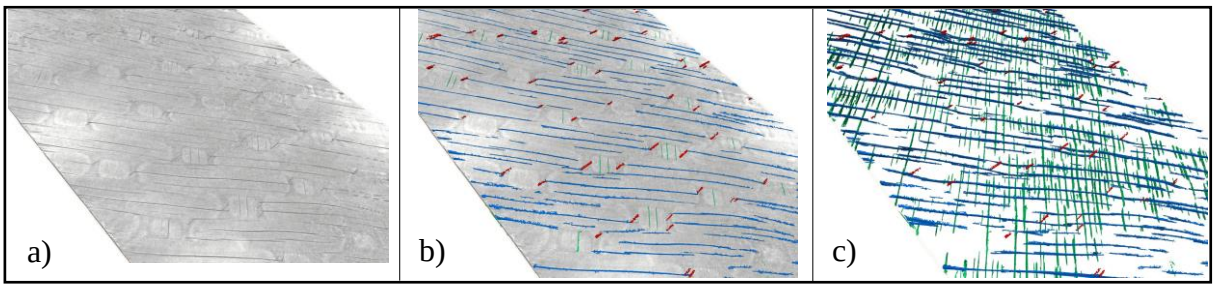

Figure 7. Segmentation process: a) start 3D image, b) image after segmentation process and c) only segmented cracks.

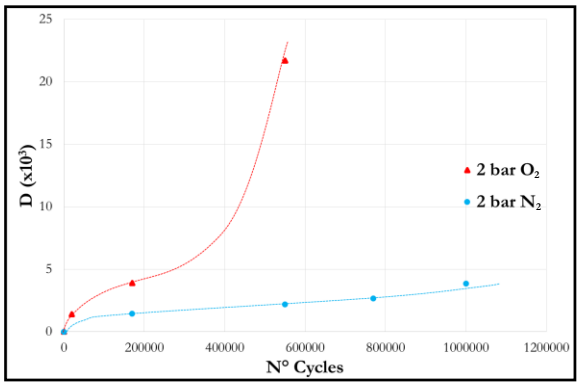

Figure 8. Evolution of the damaged volume ratio as a function of the number of cycles.

Fig. 10 shows the results of the segmentation process for external and internal plies for the 2 bar N_2 sample after 550k cycles. The global scenario is similar to that of 2 bar O_2 samples for external plies, where cracks randomly appear along preferential directions; on the other hand, in the internal plies, the scenario is totally different, since several cracks onset and propagate far from the edges of the specimen. As in 2 bar O_2 samples, the main contribution to damage is provided by cracks on the external surfaces. In the internal plies the amount of crack is constant up to the end of the test, while a slow rise of D is observed in the exterior plies. This scenario testifies a low impact of the environment on 2 bar N_2 samples.

In summary, no significative change in D is measured in 2 bar N_2 samples, while a continuos rise of D is observed in 2 bar O_2 samples, particularly in the proximity of the sample final failure where a sharp rise of D is noted. These results are in good accord with measures at the sample scale involving macroscopic quantities.

Excerpt from ISBN 978-3-00-053387-7

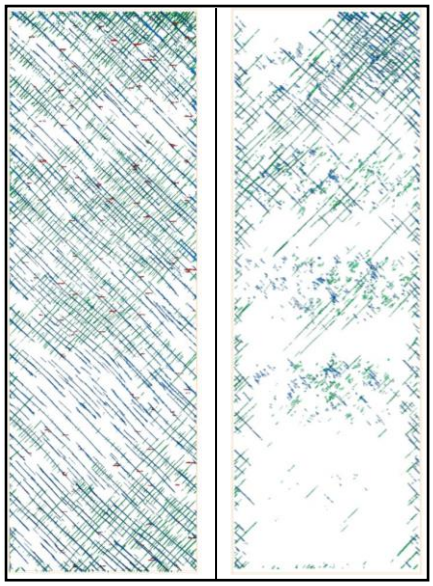

Figure 9. Segmentation result on 550k cycles 2 bar O_2: difference in amount of cracks between an external ply (left) and an interior ply (right).

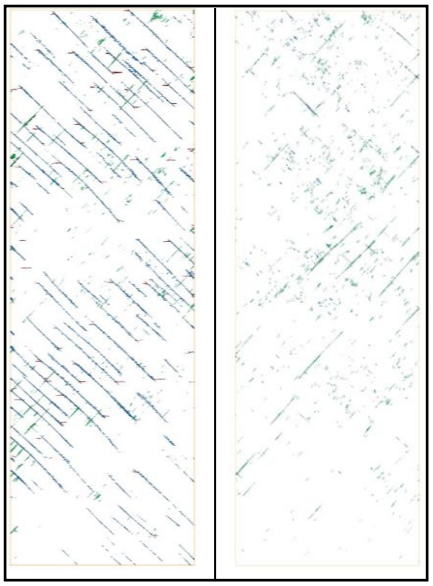

Figure 10. Segmentation result on 550k cycles 2 bar N_2: difference in amount of cracks between an external ply (left) and an interior ply (right).

4. Conclusions and perspectives

Fatigue tests in oxidizing (2 bar O_2) and inert (2 bar N_2) environment are out to investigate thermo-oxidation/fatigue interaction. Failure of the 2 bar O_2 sample occurs after 550k cycles, while the 2 bar N_2 sample has not failed after 1M cycles.
DIC measured reveals a quite different behavior for the two tested specimens after 200k-400k cycles, testifying higher degradation, decrease of Gsec modulus, as a function of number of cycles for the 2 bar O_2 sample.
According to this observation, µCT scans show a considerable rise of damage volume ratio in 2 bar O_2 samples comparatively to 2 bar N_2 samples, in the same range of number of cycles. Through µCT scans it is also shown that the two configurations exhibit consistently different damage mechanisms, the 2 bar O_2 sample being particularly prone to damage development in the external surfaces directly exposed to the oxidizing environment. In general, for both samples, the highest contribution to total damage comes from the external surfaces while internal plies are less affected by degradation.
In future studies, fatigue tests will be carried out under air at atmospheric pressure environment in order to confirm the observed trends. Moreover, a Finite Element model will be developed to better understand through comparative simulations the impact of a thermo-oxidizing environment on the observed behavior.

Acknowledgments

Part of the present research has been carried out within the context of the FUI COMPTINN' program, in collaboration with Airbus Group Innovation and SAFRAN Group. We acknowledge Aircelle, SAFRAN Group for providing the material under study. This work was partially funded by the EQUIPEX "GAP" (reference ANR-11-EQPX-0018) and LABEX "INTERACTIFS" (reference ANR-11-LABX-0017-01) French Governmental programs.

Excerpt from ISBN 978-3-00-053387-7

References

[1] V. Carvelli, J. Pazmino, SV Lomov, AE Bogdanovich, DD Mungalov, I. Verpoest, Quasi-static and fatigue tensile behavior of a 3D rotary braided carbon/epoxy composite, *Journal of Composite Materials*, 47, 3195-3209, 2013.

[2] V. Carvelli, G. Gramellini, SV Lomov, AE Bogdanovich, DD Mungalov, I. Verpoest, Fatigue behavior of non-crimp 3D orthogonal weave and multi-layer plain weave E-glass reinforced composites, *Composites Science and Technology*, 70, 2068-2076, 2010.

[3] V. Carvelli, VN Tommaselli, SV Lomov, I. Verpoest, V. Witzel, B. Van den Broucke, Fatigue and post-fatigue tensile behavior of non-crimp stitched and unstitched carbon\epoxy composites, *Composites Science and Technology*, 70, 2216-2224, 2010.

[4] K. Vallons, M. Zong, SV Lomov, I. Verpoest, Carbon composites based on multi-axial molti-ply stitched preforms – Part 6. Fatigue behavior at low loads: Stiffness degradation and damage development, *Composites*, Part A 38, 1633-1645, 2007.

[5] W. Van Paepegem, Fatigue damage in structural textile composites: testing and modelling strategies, In: *Fatigue failure of textile fibres*, Ed. M. Miraftab, 201-241, 2009.

[6] X. Colin, J. Verdu, Strategy for studying thermal oxidation of organic matrix composites, *Composites Science and Technology*, 65, 411-419, 2005.

[7] X. Colin, C. Marais, J. Verdu, Kinetic modelling of the stabilizing effect of carbon fibers on thermal ageing of thermoset matrix composites, *Composites Science and Technology*, 65, 117-127, 2005.

[8] C. Guigon, MC. Lafarie-Frenot, Y. Pannier, L. Olivier, C. Rakotoarisoa, Impact of temperature and thermal cycling ageing on performance of 3D woven composites whit polymer matrix manufactured by RTM, *Proceeding of 16th European Conference on Composite Materials (ECCM16), Seville, Spain*, June 22-26 2014.

[9] F. Bremand, M. Cottron, P. Doumalin, J.C. Dupré, A. Germaneau, V. Valle, *Mesures en mécanique par méthodes optiques*, R1850 Editions Techniques de l'Ingénieur, 2011.

[10] C. Guigon C, MC Lafarie-Frenot, Y. Pannier , C. Rakotoarisoa, Thermal cycling ageing of 3D woven polymer matrix composites, Proceeding of 19th Journees nationales sur les composites (JNC19), Lyon, France, June 29 - July 1 2015.

[11] M.C. Lafarie-Frenot, Damage mechanisms induced by cyclic ply-stresses in carbon–epoxy laminates: Environmental effects, *International journal of fatigue, 28*, 1202-1206, 2006.

[12] E. Kristofer Gamstedt, O. Redon, P. Brøndsted, Fatigue Dissipation and Failure in Unidirectional and Angle-Ply Glass Fibre/Carbon Fibre Hybrid Laminates, *Key Engineering Materials*, 221-222, 35-48, 2002.

[13] S.Topal, L. Baiocchi, AD. Crocombe, SL. Ogin, P. Potluri, PJ. Withers, M. Quaresimin, PA. Smith, MC. Poole, AE. Bogdanovich, Late-stage fatigue damage in a 3D orthogonal non-crimp woven composite: An experimental and numerical study, *Composites,* Part A 79, 155–163, 2015.

[14] SD. Pandita, G. Huysmans, M. Wevers, I. Verpoest, Tensile fatigue beaviour of glass plain-weave fabric composiotes in on- and off-axis directions, *Composites,* Part A 32, 1533-1539, 2001.

Excerpt from ISBN 978-3-00-053387-7